Journal of ELECTRICAL ENGINEERING, VOL. 58, NO. 1, 2007, 3–9

ANALYSIS OF AN AXIAL FLUX PERMANENT MAGNET MACHINE (AFPM) BASED ON COUPLING OF TWO SEPARATED SIMULATION MODELS (ELECTRICAL AND THERMAL ONES)

Eva Belicová [*] — **Valéria Hrabovcová** [**]

The paper deals with a transient thermal analysis of an air-cooled AFPM machine with a one rotor-two stators configuration. Two separated models of the machine are coupled: an electrical model and a thermal one. In calculation, the change of the stator winding resistance affected by the temperature rise is taken into account. Analysis is made for a 5 kW AFPM machine.

K e y w o r d s: axial flux permanent magnet machine thermal analysis, thermal network model, electrical simulation model, temperature rise, thermal resistance

1 INTRODUCTION

During the last decade a significant development of permanent magnet materials as well as improvement of their properties have been achieved. Applications for permanent magnet materials have been also found in electrical machines. The progressive evolution of diverse kinds of permanent magnet materials has shown that it is necessary to focus on the thermal stability of the permanent magnets and, of course, on the sensitivity of specific permanent magnet parameters to the rise of temperature.

A lot of researchers have concentrated their interest on the thermal behaviour of electrical machines during operation to identify the causes of motor's failure. Most attention was given to induction machines in the past. Recently, machines with permanent magnets have been more and more popular because they give the possibility to decrease the motor size abreast with increasing their qualitative parameters.

When electrical machines are magnetized by Neodymium-Iron-Boron (Nd-Fe-B) magnets, the remanent flux density of the permanent magnet material depends on temperature, which results in a variation of the amplitude of the induced EMF and, thereby, in changes of the characteristic performance of the machine. A thermal demagnetization risk can also occur if the magnet temperature exceeds the allowed limit, which is typically between 120 and 210 °C for the Nd-Fe-B magnets nowadays. Furthermore, possibility for mechanical hazards could occur if permanent magnets are glued on the surface of the rotor disk and the temperature of the glue joint exceeds a critical value. An accurate value of the phase resistance which also depends on temperature is required in order to find correctly Joule losses. Thus it is very useful to estimate the operation temperature of the phase winding and of the permanent magnets during transient analysis to find out the thermal time constant and so make recommendations for machine long-time operation. The analysis is made for a low-speed interior-rotor axial flux permanent magnet machine with surface mounted magnets.

Previously, a thermal model for the motor under investigation was developed for the steady state analysis in [1]. In the present paper the analysis is extended to make transient analysis. Simulation is made to gain the heating curves of individual parts of the machine if the motor is loaded by the nominal torque.

The final simulation model represents a coupled electrical model of the machine with its thermal model to take into account changing machine parameters with temperature variation, mainly the well known temperature dependence of the stator resistance.

2 SIMULATION MODEL

The simulation model was created to make transient thermal analysis of the machine operated under constant full load including individual parameter changes affected by the change of temperature. The stator resistance is sensitive to temperature variation and hence the stator current and Joule losses change. These losses represent one of the sources for the thermal model, where the temperature is investigated in individual parts of the machine.

Further, some thermal resistances change their values with temperature because of thermal variation of thermal conductivity of the used construction material, especially if air cooling is considered and the internal space of the

[*] VUJE a.s, Trnava, Okružná 5, 91864, Trnava, E-mail: eva.belicova@gmail.com; [**] University of Žilina, Faculty of Electrical Engineering, Univerzitná 8215/1, 010 26 Žilina, Slovakia; E-mail: valeria.hrabovcova@fel.utc.sk

ISSN 1335-3632

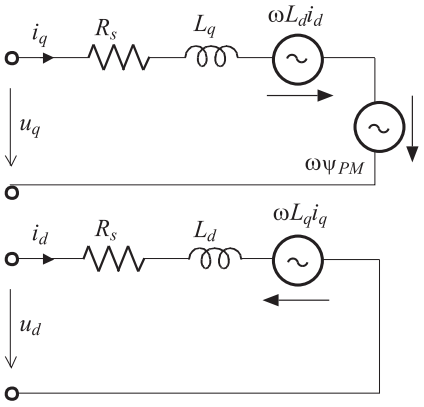

Fig. 1. Equivalent circuit of AFPM in d and q axis.

machine is also filled by air. The heat transfer factor is dependent on temperature rise, too. Both electrical and thermal simulation models will be described below.

2.1 Electrical Simulation Model

Electrical simulation model is based on equations of the general theory of AC electrical machines transformed to the $d, q, 0$ reference frame. An equivalent circuit of AFPM considering the linkage PM flux ψ_{PM} is shown in Fig. 1. Its main advantage is that the reference frame is identified with the rotor and so the rotor parameters and equations need not be transformed. Further, it is very important to choose suitable transformation constants to keep the invariance principle of powers. It has been chosen as $k_d = k_q = \sqrt{2/3}$.

The input phase voltages given as

$$\begin{aligned} u_a &= U_{\max} \sin \omega_s t \,, \\ u_b &= U_{\max} \sin(\omega_s t - 2\pi/3) \,, \\ u_c &= U_{\max} \sin(\omega_s t + 2\pi/3) \end{aligned} \tag{1}$$

are transformed to d, q axes by the well known Park's transform and after some modifications the final equations are given as

$$\begin{aligned} u_d &= \sqrt{3/2} U_{\max} \sin(\omega_s t - \vartheta_r) \,, \\ u_q &= \sqrt{3/2} U_{\max} \cos(\omega_s t - \vartheta_r) \end{aligned} \tag{2}$$

where $U_{\max}$, ω_s, ϑ_r are the amplitude of phase voltage, synchronous angular speed, and rotor position, respectively.

The complete system of equations for AFPM which describe the electrical simulation model for transient and steady state analysis is

$$u_d = R_s i_d + L_d \frac{\mathrm{d}i_d}{\mathrm{d}t} - \omega L_q i_q \,, \tag{3}$$

$$u_q = R_s i_q + L_q \frac{\mathrm{d}i_q}{\mathrm{d}t} + \omega L_d i_d + \omega \psi_{PM} \,, \tag{4}$$

$$m_e = p\left[(L_d i_d + \psi_{PM}) i_q - (L_q i_q) i_d\right] \,, \tag{5}$$

$$J \frac{\mathrm{d}\omega}{\mathrm{d}t} = p(m_e - m_L) \,, \tag{6}$$

$$\vartheta_r = \int \omega_r \mathrm{d}t \,, \tag{7}$$

$$\vartheta_L = \vartheta_r - \omega_s t \tag{8}$$

where the synchronous angular speed is given as

$$\omega_s = 2\pi f_s \tag{9}$$

and ϑ_L is the load angle of the machine, ω_r is the electrical angular speed of the rotor, R_s is the stator resistance, L_d and L_q are synchronous inductances in d and q axes, m_e is the electromagnetic torque, m_L is the load torque, J is the moment of inertia, p is the number of pole pairs and f_s is the supply frequency. The speed of the rotor is then calculated from ω_r as

$$n = \frac{60\omega_r}{2p\pi} \,. \tag{10}$$

The linkage PM flux transferred to the $d, q, 0$ reference frame is given by

$$\psi_{PM} = \sqrt{\frac{3}{2}} \frac{U_{\max}}{\omega_N} \,, \tag{11}$$

where ω_N is the electrical angular speed of the machine operated under no load condition.

To obtain the actual stator current in one phase it is necessary to perform inverse Park's transformation. It is given as

$$i_s = \sqrt{2/3} i_d \cos(\vartheta_r) - \sqrt{2/3} i_q \sin(\vartheta_r) \,. \tag{12}$$

The other phase currents are shifted by $120°$.

This simulation model was used for determination of the root-mean-square value of the stator current to calculate Joule losses in the stator winding and, in combination with the thermal simulation model, the change of the stator resistance with changing winding temperature was taken into account.

2.2 Thermal Simulation Model

In the thermal network model used for simulation of thermal phenomena the investigated object is divided into several thermal elements that are represented by a node configuration (usually one node and some thermal resistances). The elements are linked together, forming a network of nodes and thermal resistances, see Fig. 2. The thermal network is similar to an electrical network consisting of current sources and resistances. For an air-cooled AFPM the ambient air temperature is usually taken as a thermal reference value θ_a.

A transient thermal simulation model was built to gain the heating curves of individual parts of the machine such as stator yoke, teeth, machine frame, winding and so

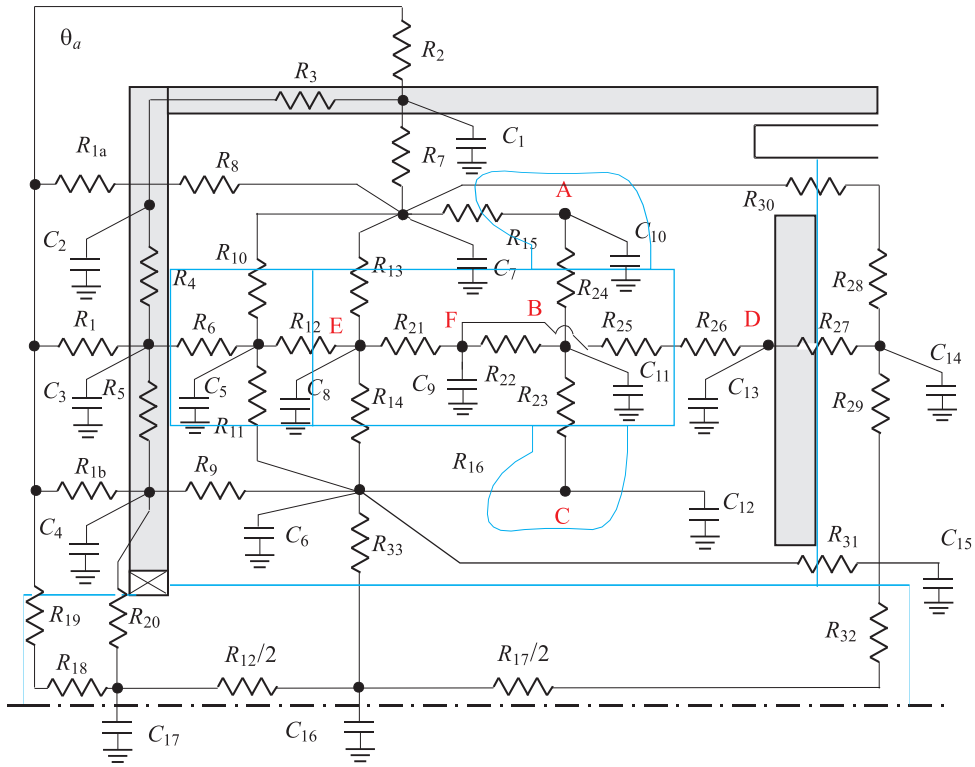

Fig. 2. Simplified thermal network of analyzed AFPM.

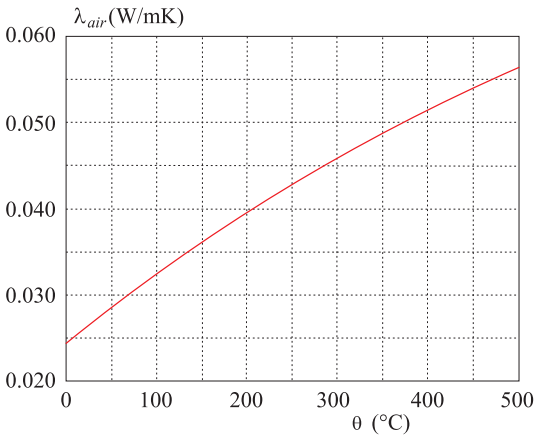

Fig. 3. Thermal conductivity of the air versus temperature according to [6].

on. Simulation was made for transient at a constant full load condition and it is based on the following differential equation:

$$\frac{\mathrm{d}}{\mathrm{d}t}(\Delta\boldsymbol{\theta}) = \mathbf{C}^{-1}\left(\Delta\mathbf{P}_d - \mathbf{G}(\Delta\boldsymbol{\theta})\right). \tag{13}$$

Here $\Delta\mathbf{P}_d$ is the loss vector containing the dissipated losses assigned to each node and $\Delta\boldsymbol{\theta}$ is the temperature rise vector given as follows:

$$\Delta\mathbf{P}_d = [\,\Delta P_{d1} \quad \Delta P_{d2} \quad \ldots \quad \Delta P_{dn}\,]^\top, \tag{14}$$

$$\Delta\boldsymbol{\theta} = [\,\Delta\theta_1 \quad \Delta\theta_2 \quad \ldots \quad \Delta\theta_n\,]^\top. \tag{15}$$

$\mathbf{G}$ is the conductance matrix defined as

$$\mathbf{G} = \begin{bmatrix} \sum_{i=1}^{n}\frac{1}{R_{1,i}} & -\frac{1}{R_{1,2}} & \cdots & -\frac{1}{R_{1,n}} \\ -\frac{1}{R_{2,1}} & \sum_{i=1}^{n}\frac{1}{R_{2,i}} & \cdots & -\frac{1}{R_{2,n}} \\ \vdots & \vdots & \ddots & \vdots \\ -\frac{1}{R_{n,1}} & -\frac{1}{R_{n,2}} & \cdots & \sum_{i=1}^{n}\frac{1}{R_{n,i}} \end{bmatrix}, \tag{16}$$

where $\sum_{i=1}^{n}\frac{1}{R_{1,i}}$ is the sum of thermal conductances $1/R_{th}$ connected to a particular node.

The thermal resistances R_{th} in a thermal conductance matrix may be classified into two main following categories:

- thermal resistances due to convection and radiation on the surfaces,
- thermal resistances due to conduction inside the solids.

The value of R_{th} is related to the thermal conductivity λ_i of the material. The expression is given as

$$R_{th} = \frac{l_i}{\lambda_i S_i}, \tag{17}$$

where l_i is the length of a particular path described by a thermal resistance and S_i is the area of heat transfer.

Thermal conductivities for the solids used in electrical machines can be considered to be constants with respect to temperature. Table 1 gives some typical values for the thermal conductivities of solid materials used for analyzed AFPM.

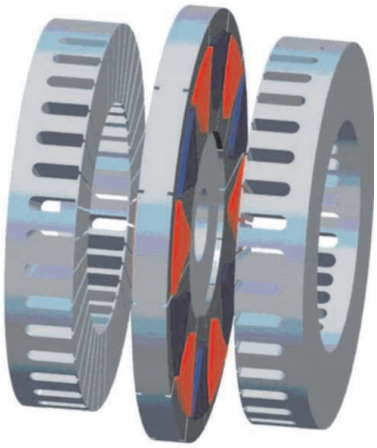

Fig. 4. Structure of AFPM, in which one rotor is located between two stators.

Table 1. Physical material thermal data

Material	λ (W/mK)	C_p (J/kgK)	ρ (kg/m^3)
Electrical steel M600-50 (in plane)	38.7	460	7600
Cu	395	390	8900
Permanent magnet (Nd-Fe-B)	9	502	7500
Slot insulation material	0.2		
Rotor disk	50	460	7800
Frame material	50	460	7800

The heat transfer from a particular surface to the ambient may be described by a thermal resistance which takes into account radiation and convection heat transfer phenomena. With a known surface area and a known heat transfer coefficient, the corresponding thermal resistance for the particular surface is given by

$$R_{th,surf} = \frac{1}{\alpha_i S_i}\,, \tag{18}$$

where α_i is the heat transfer coefficient and it is also dependent on temperature rise $\Delta\theta$. Its correct value must be found by iteration.

In Eq. 13, representation of the stored energy in the system is introduced as thermal capacitances C_{th} [3]. Each node is assigned by a thermal capacitance calculated from geometrical and material data. An element consisting of several parts has the thermal capacity given as

$$C_{th} = \sum_{i=1}^{k} m_i c_i\,, \tag{19}$$

where m_i is the mass of part i and c_i is the specific heat of part i. The equation system (13) requires a thermal capacitance matrix which is defined as:

$$C = \begin{bmatrix} C_{th1} & 0 & \dots & 0 \\ 0 & C_{th2} & \dots & 0 \\ \vdots & \vdots & \ddots & 0 \\ 0 & 0 & \dots & C_{thn} \end{bmatrix}. \tag{20}$$

Temperature dependent elements of thermal resistances in conductance matrix (16) and loss vector (14) require iterative solution because of their dependence on temperature. Therefore the elements of the matrix must be updated regularly, see Fig. 5. Especially the thermal resistances of the parts filled with air are sensitive to temperature changes because air thermal properties are considerably depending on temperature, see Fig. 3. All changes have been taken into account and properly implemented during simulation to the model equations.

Thermal resistances were calculated according to the type of heat transfer, such as conduction, convection and radiation. How to calculate individual thermal resistances was described in detail in [1].

The electrical and thermal simulation models were coupled together to account for almost all changes created in AFPM by temperature variations. The electrical simulation model was used to determine the values of root-mean-square current I_{RMS} at a certain value of R_s given by actual temperature. The thermal model was used to determine the temperature rise in individual nodes and after adding the ambient temperature value the actual temperature values were gained. In Fig. 6 there is shown the change of the stator resistance affected by temperature variation in time. Based on this current and the stator winding resistance R_s the Joule losses were calculated as follows:

$$\Delta P_d = 3 R_s I_{RMS}^2\,. \tag{21}$$

These losses were divided into three portions; stator outer endwinding losses and inner endwinding losses as well as slot part of winding losses. It was made in ratio given by the resistance value of each winding part. These losses were input to the thermal model as thermal sources. Here it must be noticed that iron losses in the stator yoke and teeth and also losses in rotor PM were kept constant during the whole simulation. Their values have been determined by expression given in [1] and [5].

Based on these sources and the whole configuration of the thermal model the temperature values were calculated in the thermal model. The outputs of the model were temperature values in 17 nodes shown in Fig. 3. The main interest was given to six nodes marked by six letters A-F. The thermal model was coupled with the electrical one through actual temperature values of stator windings that were investigated in three nodes (A-C) as mentioned before. Thereafter, the average temperature was calculated and used to determine a new value of stator resistance by expression

$$R_s = R_{s\theta a}\left[1 + k_{Cu}(\theta - \theta_a)\right]\,, \tag{22}$$

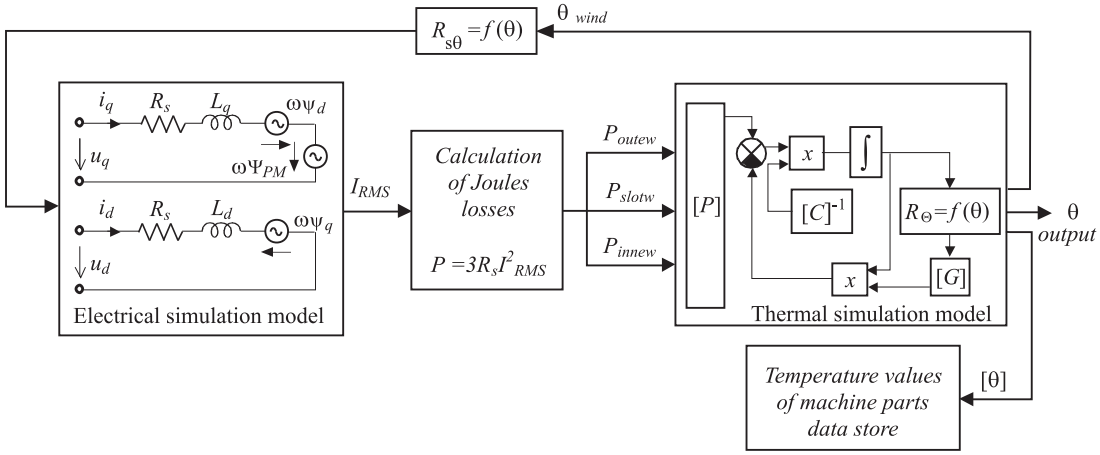

Fig. 5. Block diagram of the simulation model consisting of electrical and thermal model.

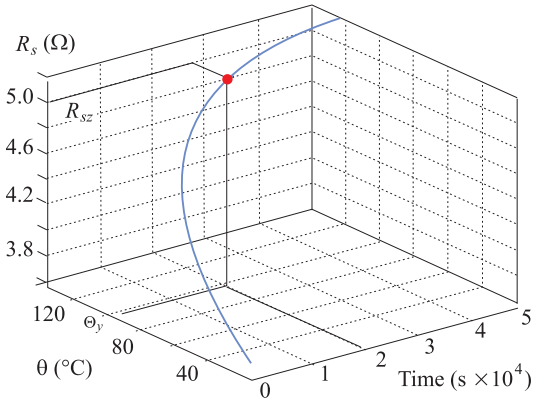

Fig. 6. The thermal change of stator resistance in time.

where k_{Cu} is the temperature factor of copper resistivity $\left(k_{Cu} = 3.8 \times 10^{-3}\,°\mathrm{C}^{-1}\right)$ [1], $R_{s\theta a}$ is the resistance at given ambient temperature θ_a and θ is the actual temperature. Then the stator resistance value in the electrical model (Eqs. 3, 4) was updated and consequently the RMS value of the stator current was updated, too. In this way, it was possible to have a portrait of the thermal changes in the machine.

3 SIMULATION RESULTS

The simulation was made for a 12-pole axial flux permanent magnet machine, construction stator-rotor-stator (see Fig. 4), the rating of which is as follows: 3-phase, 30 Hz, 5 kW, 230 V Y, 8.4 A, 300 rpm, and 159 Nm.

The simulation parameters used in equations (1)–(12) are stator resistance at 20 °C $R_{s20\,°\mathrm{C}} = 3.7\,\Omega$, synchronous inductance in d- and q-axis $L_d = 0.055\,\Omega$, $L_q = 0.06\,\Omega$, moment of inertia $J = 0.016\,\mathrm{kgm}^2$ and linkage PM flux $\psi_{PM} = 2.12$ Wb.

The thermal resistances and capacitances were calculated, as mentioned above, from machine dimensions and physical material properties given in Tab. 1 for the assumed type of heat transfer.

Both models, electrical and thermal one, were coupled together to take into account the changes of the motor parameters. Thermal capacitances were initialized according to values calculated by Eq. 19 and they were kept constant during the whole simulation. Some of these values, especially for air filled parts, could be updated during simulation. Nevertheless, it has not been considered because it did not have a significant effect. Thermal resistances were calculated in each computing step of simulation and so they were regularly updated. It was done with regard to the thermal variations of the construction material properties. A block diagram of the whole simulation model is shown in Fig. 5.

The electrical model was coupled with the thermal one through temperatures investigated in the nodes corresponding to outer and inner endwindings as well as to the slot part of the winding. From these values the overall stator resistance was computed as it is shown in Fig. 6. One can see the time change of the stator resistance R_s affected by changing temperature. As an example there is marked one point on the curve, which corresponds to the value of the stator resistance R_{sz} according to the actual stator winding temperature θ_y at given simulation time t_x. The RMS value of the stator current was investigated while respecting the stator resistance changes to calculate Joule losses. They are displayed in Fig. 7 in greater details. There are illustrated losses in individual parts of the winding, the values of which have been sources for the thermal model. The peak values in the Joule losses waveform are caused by sensitivity of the electrical simulation model to any changes of parameters used during simulation. The iron losses in the stator and losses in the PM were kept constant ($\Delta P_{Fe,teeth} = 24$ W, $\Delta P_{Fe,yoke} = 7$ W, $\Delta P_{PM} = 6$ W).

When the variation of Joule losses was known, the temperature values in individual parts of the machine could be computed. The main interest was focused on investigation of the temperatures in the nodes corresponding to the stator teeth, stator yoke, permanent magnets, outer

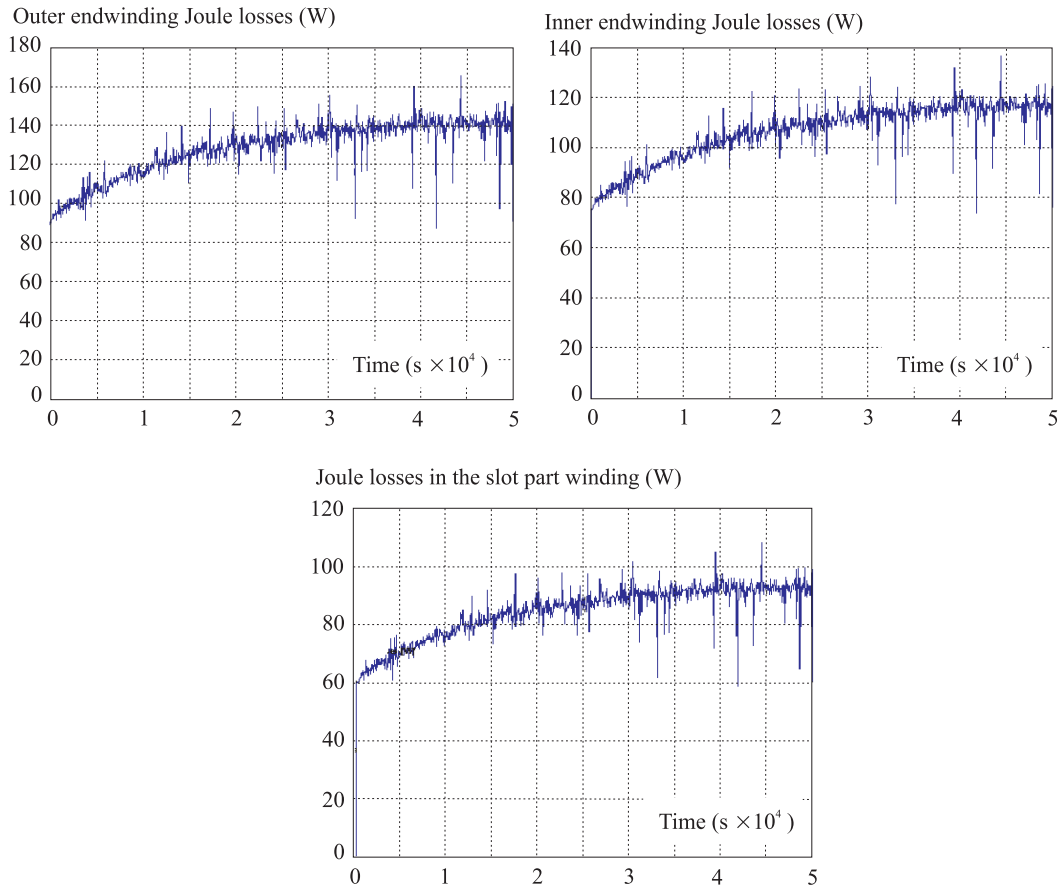

Fig. 7. Joule losses in outer endwinding, inner endwinding and int the slot part of winding

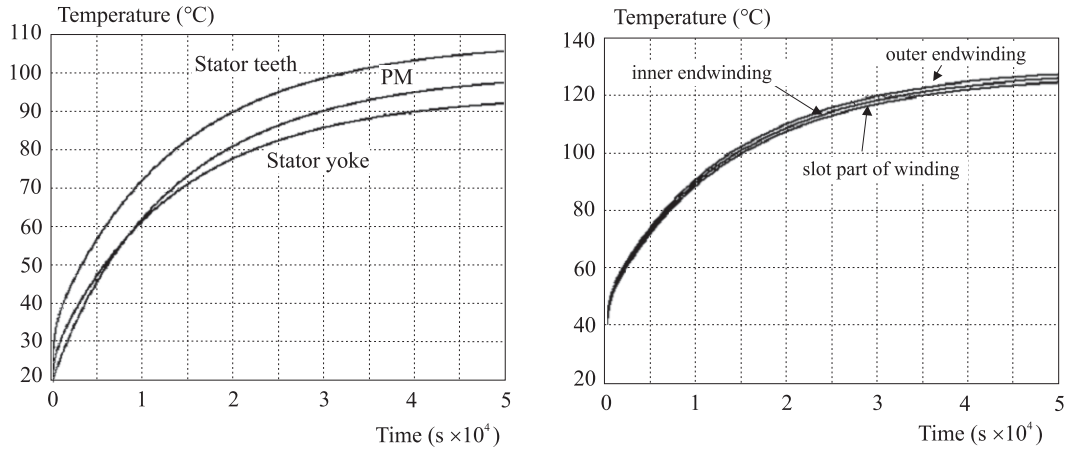

Fig. 8. Simulated temperature in analyzed nodes.

endwinding, inner endwinding and slot part of winding how and it is shown in Fig. 8.

The heating curves of the simulated motor were also measured for the constant full load condition and the results were published in [4] for transient analysis and in [1] for steady state analysis. The comparison (see Fig. 9) says that acceptable coincidence has been achieved. The permanent magnet temperature is illustrated by one point because PM temperature was not measured during machine operation. However, the final value of PM temperature was gained immediately after stopping the machine. The temperature was about 102 °C. Based on this value it can be said that PM are not in danger because this value has not overstepped the limit values mentioned above. Here it must also be noticed that heat rating of the insulation is of class B for which the limit temperature is 170 °C if air is used as a coolant.

The simulation was performed in Matlab-Simulink for 50000 seconds, which is almost 14 hours with a variable computing step using the Adams numerical method and

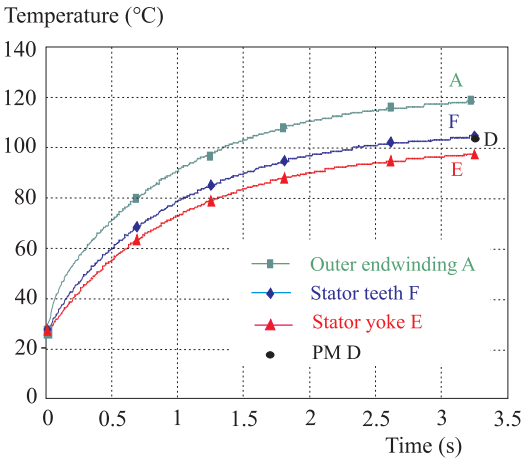

Fig. 9. Measured temperatures in nodes marked by letters A, D, E and F in Fig.2.

the consumed time was about 50 hours on a computer with processor Intel Pentium 2.8 GH and 2 GB RAM. The simulation time was quite long but it could give relevant information about AFPM behaviour from the point of view of the thermal analysis. This simulation method was chosen to study the behaviour of AFPM at various loadings during various operation duties like a short time duty, intermittent duty or overloading. This simulation model can be used to gain the heating of PM during the pre-manufacturing period of such a kind construction of machine as it is analyzed here to make sure that demagnetization risk caused by the rise of temperature will not occur during operation.

4 CONCLUSION

This paper deals with a transient analysis of an air-cooled axial flux permanent magnet machine (AFPM). The simulation was made by coupling an electrical simulation model with a thermal network simulation model.

The electrical simulation model has been built in Simulink on the basis of differential equations to obtain the stator current waveform. The RMS value of the stator current was determined from the stator current waveform and this value of current was used to find out Joule losses in the stator winding which were used as sources for thermal network model of AFPM. Stator resistance variation caused by the change of winding temperature was taken into account.

Then the thermal network model was built and used in transient simulation to gain the heating curves. The temperature values were investigated in 17 nodes shown in Fig. 2. The main importance was set onto 6 nodes marked by letters A-F. During simulation, the thermal resistances have been calculated according to temperature variation of the thermal conductivity factors and so the thermal model was iteratively updated. The final value of the temperature was used for stator resistance correction in the electrical simulation model to gain the right waveform of the stator current. In such a way both models have been completed.

Simulated results are in acceptable coincidence with measurements and so it can be said that this simulation model is suitable for gaining the probable thermal behaviour of AFPM. Otherwise, this simulation is a very time consuming way how to get this behaviour of the machine. Also it is true that this way of investigation is very exacting for computer computation possibility.

Acknowledgement

This work was supported by the Science and Research Assistance Agency under the contract No. APVT-20-039602 and by the Scientific Grant Agency of the Ministry of Education of SR and the Slovak Academy of Science VEGA under contracts No. 1/2052/05 and 1/3086/06.

References

[1] PARVIAINEN, A.: Design of Axial-Flux Permanent-Magnet Low-Speed Machine and Performance Comparison between Radial-Flux and Axial-Flux Machines, Dissertation Thesis, Lappeenranta University of Technology, 2005.

[2] KYLANDER, G.: Thermal Modelling of Small Cage Induction Motors, Ph.D. Thesis, Chalmers University, 1995.

[3] LINDSTRÖM, L.: Thermal Model of a Permanent Magnet Synchronous Motor for a Hybrid Electrical Vehicle, Department of Electric Power Engineering Chalmers University of Technology Gtenborg, Sweden, April 1999.

[4] BELICOVÁ, E.—HRABOVCOVÁ, V.—PARVIAINEN, A.: Transient Thermal Modelling of Axial Flux Permanent Magnet Machines-Verification of the Theoretical Assumptions by Measurements, ISEM 2005, Praha, 2005.

[5] GERIAS, J. F.—WNAG, R.-J.—KAMPER, M. J.: Axial Flux Permanent Magnet Brushless Machines, Kluwer Academic Publishers, Netherlands, 2004.

[6] http://www.engineeringtoolbox.com/air-properties- d_156.html.

Received 12 June 2006

Eva Belicová (MSc, PhD), graduated in electrical engineering from the University of Žilina, and gained her PhD in electrical machines and instruments from the University of Žilina in 2006. Now she is with VUJE Inc. in Trnava.

Valéria Hrabovcová (Prof, MSc, PhD), graduated in electrical engineering from the University of Žilina, in Žilina and gained her PhD in electrical engineering from the Slovak University of Technology in Bratislava in 1985. She is a professor of electrical machines at the University of Žilina, Faculty of Electrical Engineering at undergraduate and postgraduate levels. Her professional and research interests include electronically commutated electrical machines.